J|A|C|S
JOURNAL OF THE AMERICAN CHEMICAL SOCIETY

Communication

pubs.acs.org/JACS

Synthesis and Characterization of a p-Type Boron Arsenide Photoelectrode

Shijun Wang,† Sarah F. Swingle,† Heechang Ye, Fu-Ren F. Fan, Alan H. Cowley, and Allen J. Bard*

Center for Electrochemistry, Department of Chemistry and Biochemistry, The University of Texas at Austin, Austin, Texas 78712, United States

Supporting Information

ABSTRACT: A p-type boron arsenide photoelectrode was prepared from a material consisting of a thin layer of boron arsenide on a boron substrate. The structure of the material was identified using X-ray diffraction and scanning electron microscopy, and the surface composition was determined by means of X-ray photoelectron spectroscopy. The electrode was found to be photoactive under both visible light and UV−vis irradiation and displayed a photocurrent of ~0.1 mA/cm^2 under UV−vis irradiation at an applied potential of −0.25 V vs Ag/AgCl. Mott−Schottky plots for this boron arsenide electrode displayed an estimated flat-band potential near the onset photopotential. The estimated indirect band gap, as determined from incident photon-to-electron conversion efficiency plots, is 1.46 ± 0.02 eV.

We report the synthesis and characterization of a p-type boron arsenide (BAs) photoelectrode that is suitable for photoelectrochemical (PEC) applications. X-ray diffraction (XRD) and scanning electron microscopy (SEM) were used to characterize the structure of a representative BAs crystal, the surface composition of which was analyzed by means of X-ray photoelectron spectroscopy (XPS). To the best of our knowledge, neither the PEC nor the photovoltaic (PV) properties of BAs have been reported previously.

Compound main-group semiconductors such as gallium arsenide (GaAs) possess several electronic properties that are superior to those of silicon, thus making them suitable for a variety of novel applications.[1] BAs is of particular interest in this context because it is isoelectronic with Si and has good prospects for PV and PEC applications. Interestingly, however, it has long been neglected in the study of compound main-group semiconductors. BAs is the most covalent of the family of III−V compounds, and theoretical investigations have revealed that boron may even act as the anion in this nearly perfectly covalent compound.[2] Moreover, it is stable against chemical decomposition and dissolution.[3] A further interesting feature is that the valence bands of BAs and GaAs are offset, thus potentially offering an ideal alloying system.[4]

Various approaches to the synthesis of BAs starting from the elements were reported several decades ago. For example, heating equimolar quantities of boron and arsenic in a sealed, evacuated quartz tube at 800 °C resulted in the formation of a cubic form of BAs with unspecified stoichiometry.[5] An unknown orthorhombic phase, subsequently identified as $B_{12}As_2$, was described in the same report and was formed by evaporation of arsenic from cubic BAs at temperatures greater than 920 °C.[5] In a different approach, elemental boron and arsenic were located at opposite ends of an evacuated sealed silica tube. The two ends of the vessel could be heated independently. For example, with boron heated at 700−800 °C and arsenic pressures in excess of 1 atm, a cubic material was isolated with a boron-to-arsenic mole ratio close to unity. On the other hand, with a boron temperature of 1000−1100 °C and arsenic pressures less than 1 atm, compounds with boron-to-arsenic mole ratios of 5−7 to 1 were isolated and corresponded to compositions in the range $B_{6-7}As$.[6] Cubic BAs has also been prepared using a boron-to-arsenic mole ratio of 1 to 2−2.5 at 1200 °C under a pressure of 4−5 kbar. The BAs was isolated from unreacted arsenic by treatment with hot nitric acid, which oxidatively attacks arsenic preferentially.[3]

In the present work, BAs was prepared via the reaction of boron powder with an excess of elemental arsenic in sealed, evacuated quartz tubes that were heated to 800 °C. Additional information regarding the syntheses of these BAs samples is provided in the Supporting Information (SI). The reaction of equimolar quantities of these elements was found to produce a material that is deficient in arsenic. As summarized in Table 1, systematic studies of the variation of the boron-to-arsenic mole ratio revealed that it is necessary to use an arsenic-to-boron mole ratio of 1.90 to 1 in order to produce a material with the desired 1:1 stoichiometry. In the final product there were clearly also crystals identified as elemental As. Treatment of this product with hot nitric acid could remove these but was found to result in a material with a diminished photocurrent. Hence, in the present work, the excess arsenic was removed manually. The XRD and XPS data for this material are provided in

Table 1. Molar Equivalents of Arsenic Used for the Synthesis of BAs (The Product Analyses Are Based on XPS Data)

$B + xAs \rightarrow BAs_y$

reactant (x)	product (y)
1.00	0.569
1.22	0.753
1.44	0.794
1.90	0.993
2.54	1.213

Received: February 22, 2012
Published: June 21, 2012

ACS Publications © 2012 American Chemical Society

dx.doi.org/10.1021/ja301765v | *J. Am. Chem. Soc.* 2012, 134, 11056−11059

Figures S1 and S2 in the SI, respectively. XPS quantification data are provided in Table S1 in the SI.

For use in PEC applications or to study the semiconductor properties, it is necessary to have the stoichiometry close to 1:1 and a level of impurities (dopants) in the sub-ppm range. Because of the difficulty in preparing a BAs electrode from a powder sample, granular boron (0.42−4.75 mm) was treated with 2 molar equiv of arsenic under conditions similar to those described above. Additional information regarding the syntheses of these BAs samples is provided in the SI. SEM images of the product, which are displayed in Figure 1, revealed that an interesting surface reaction had taken place, resulting in the deposition of a thin layer of BAs on top of the boron substrate. The BAs thin layer was not continuous and showed gaps where the boron core was clearly visible.

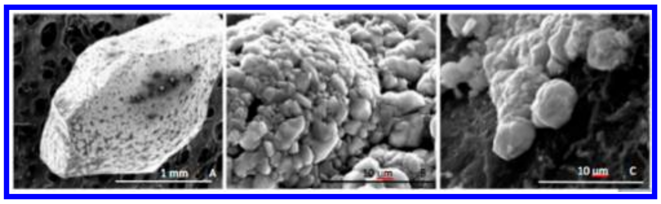

Figure 1. SEM images revealing the surface and core structure of the BAs-containing material prepared from granular boron. (A) A single piece of BAs. (B) Area of continuous BAs surface coverage. (C) Area featuring a gap in the surface coverage. The light material is BAs and the dark material is the boron substrate.

As shown in Figure 2, the presence of polycrystalline BAs and elemental boron was established on the basis of XRD data taken from a single piece of the material.

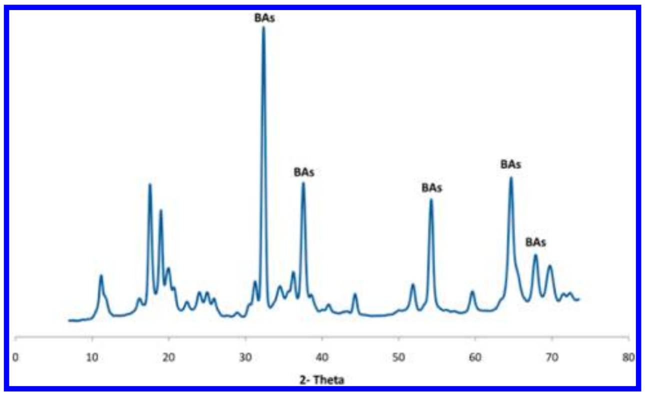

Figure 2. XRD data confirming the presence of both BAs and elemental boron in a single piece of the material prepared from granular boron. The peaks without labels are due to elemental boron.

An XPS analysis was performed to determine the chemical composition of the new BAs material. The boron 1s and arsenic 3d peaks are displayed in Figure 3. Because of the exposure of the boron core, it was not possible to determine a reliable mole ratio of the BAs thin layer in the new material. However, the high-resolution XPS spectra revealed a mole ratio of boron and arsenic close to unity, thus indicating broad coverage of the boron substrate by the BAs thin layer. The weak peak at 43−46 eV in the arsenic 3d spectrum is characteristic of an arsenic oxide.[7] XPS analysis of the boron starting material revealed the presence of oxygen, suggesting that the starting material was a possible source of the oxide contamination.

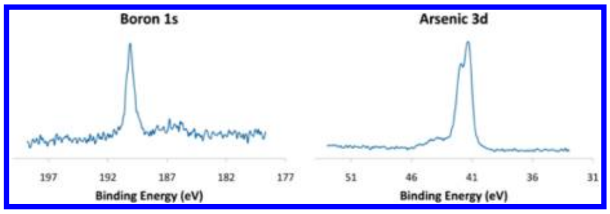

Figure 3. High-resolution XPS spectra of the BAs material prepared from granular boron. The experimental boron-to-arsenic ratio was 1 to 0.989, after correction for the atomic sensitivities. Quantification data are provided in Table S2.

A gold layer with a thickness of ∼200 nm was deposited on one side of a single piece of a BAs crystal plate of the type described above with a size of ∼3 mm. The gold deposition was accomplished by means of a commercial gold alloy electroplating solution (SG-50, Transene Co., Inc., Rowley, MA) in a two-electrode system by applying a potential of −1.0 V at BAs relative to the counter electrode. Silver epoxy paste was used to connect a copper wire to the gold layer. The copper wire and the silver epoxy paste were covered with silicone cement, resulting in a BAs electrode with an active surface area of 1 mm^2. A typical BAs photoelectrode is shown in Figure S3.

This BAs electrode displayed p-type behavior and was photoactive under both visible-light (λ > 420 nm) and UV−vis (Xe lamp) irradiation, as demonstrated by the linear sweep voltammograms (LSVs) displayed in Figure 4. The LSVs spanned a potential range of 0.0 to −0.5 V vs Ag/AgCl at a scan rate of 20 mV/s. The light source was a 150 W Xe lamp. The voltammetric measurements, which were carried out in a 0.1 M aqueous Na_2SO_4 solution containing 0.01 M methyl viologen (MV^{2+}), showed a cathodic photocurrent attributable to the reduction of MV^{2+}. The response to continuous visible-light and UV−vis irradiation is shown in Figure 4A. Figure 4B,C displays the corresponding current−potential curves for a BAs

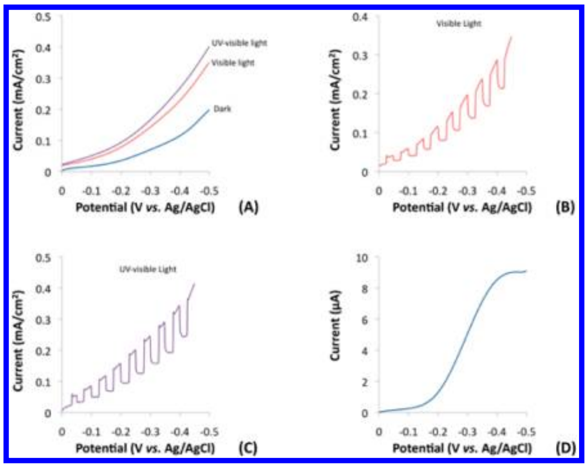

Figure 4. LSVs in a 0.1 M aqueous Na_2SO_4 solution containing 0.01 M methyl viologen. The potential was swept from 0.0 to −0.5 V vs Ag/AgCl at a scan rate of 20 mV/s. The incident light intensity at the electrode surface was 100 mW/cm^2. (A) Current flow for the new BAs material in the dark, under visible light and UV−vis irradiation. (B) Current flow for the BAs material under chopped visible light irradiation. (C) Current flow for the BAs material under chopped UV−vis irradiation. (D) LSV of an As-doped boron electrode in the dark.

crystal using chopped visible light and UV−vis irradiation, respectively.

The origin of the dark current from the BAs crystal is still not clear and requires further investigation, although an As-doped boron electrode prepared as described in the SI exhibited a dark current, as shown in Figure 4D. However, no photocurrent was detected with this electrode under the conditions described in Figure 4A−C. As shown in Figure 5 and Figure S4, the net photocurrent (after subtraction of the dark current) was ∼0.1 mA/cm^2 under full Xe lamp irradiation at an applied potential of −0.25 V vs Ag/AgCl.

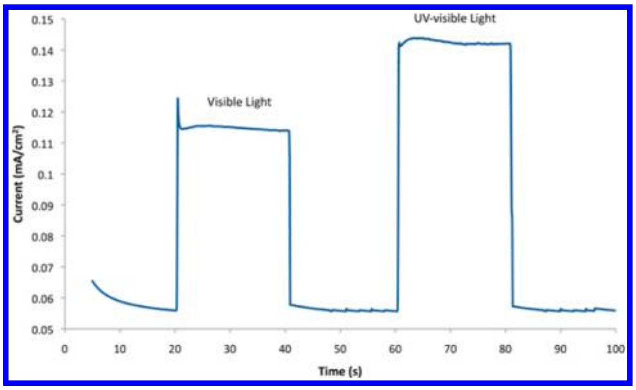

Figure 5. Current at an applied potential of −0.25 V vs Ag/AgCl in the dark (0−20 s, 40−60 s, and 80−100 s), under visible-light ($\lambda > 420$ nm) irradiation (20−40 s), and under UV−vis (Xe lamp) light irradiation (60−80 s).

Mott−Schottky plots obtained for this BAs electrode in the potential range of interest (200 Hz to 1 kHz) are provided in Figure S5. Although there was a significant shift in the plots with frequency, the estimated flat-band potential appears to be ∼0.5 V vs Ag/AgCl. Mott−Schottky plots are best applied to smooth, uniform films. For this reason, the flat-band potential was also estimated by measuring the onset photopotential. An LSV spanning the potential range from 0.45 to −0.4 V vs Ag/AgCl (Figure 6) revealed that the onset photopotential of the p-type BAs electrode in a 0.1 M aqueous Na_2SO_4 solution containing 0.01 M methyl viologen is ∼0.35 V vs Ag/AgCl.

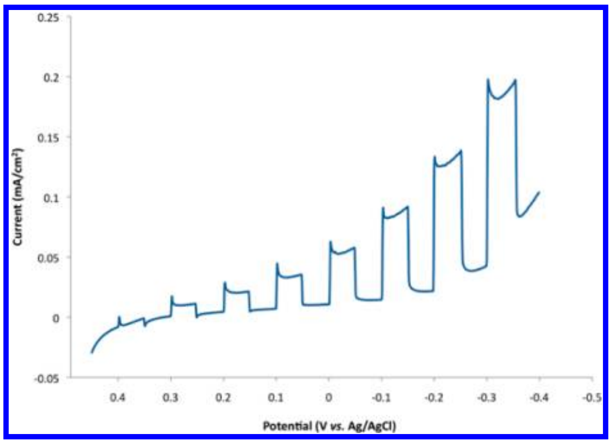

Figure 6. Overall current of a BAs electrode in a 0.1 M aqueous Na_2SO_4 solution containing 0.01 M methyl viologen under chopped UV−vis irradiation. The incident power at the electrode surface was 100 mW/cm^2.

The photocurrent for the BAs crystal was measured as a function of wavelength over the range 350 to 850 nm using a Xe lamp and a monochromator. The incident photon-to-electron conversion efficiencies (IPCEs) were calculated using the following equation:

$$\text{IPCE} = 1240\left(\frac{i_{\text{ph}}}{\lambda P_{\text{in}}}\right) \times 100\%$$

In the above equation, i_{ph} is the net photocurrent (in mA) measured at −0.25 V vs Ag/AgCl, λ is the wavelength (in nm), and P_{in} represents the incident light intensity (in mW) at the surface of the semiconductor electrode. The IPCE plot is displayed in Figure 7.

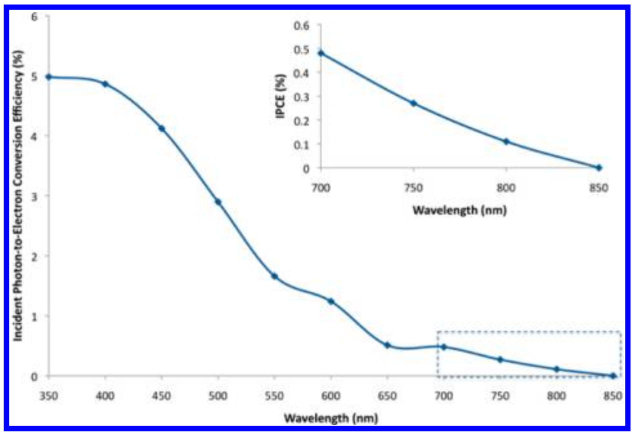

Figure 7. IPCE from a BAs crystal calculated from the net photocurrent (the overall current minus the dark current) at −0.25 V vs. Ag/AgCl in a 0.1 M aqueous Na_2SO_4 solution containing 0.01 M methyl viologen. The inset shows the marked box on an expanded scale.

The calculated IPCE reached ∼5% at 400 nm for the selected BAs crystal. The IPCE decreased with increasing wavelength and reached zero at ∼850 nm. As a consequence, the estimated indirect band gap[8,9] is 1.46 ± 0.02 eV (see Figure S6), which agrees well with the literature values[10,11] and values derived from theoretical calculations.[2,4,12,13]

Alternative methods of preparing BAs are being explored at the present time with the objective of identifying the conditions necessary to enhance the performance of this interesting semiconductor. For example, the synthesis of small molecules featuring labile ligands and σ bonds between boron and arsenic centers are being evaluated. The labile ligands are expected to undergo facile β-hydride elimination in a fashion that has been demonstrated previously.[1] The robust σ bonds between boron and arsenic are expected to promote stoichiometric control of the ligand-elimination reactions. Once a suitable precursor has been synthesized, BAs film growth by thermal decomposition of the precursor will be explored.

■ ASSOCIATED CONTENT

Ⓢ Supporting Information

Additional experimental details and XRD, XPS, and PEC data. This material is available free of charge via the Internet at http://pubs.acs.org.

AUTHOR INFORMATION

Corresponding Author
ajbard@mail.utexas.edu

Author Contributions

†S.W. and S.F.S. contributed equally.

Notes

The authors declare no competing financial interest.

ACKNOWLEDGMENTS

This work was supported by the National Science Foundation (CHE 0934450) and the Petroleum Research Fund of the American Chemical Society (48813-ND10). The XRD data were collected on instrumentation purchased with funds provided by the National Science Foundation [CHE(CRIF) 0741973].

REFERENCES

(1) Malik, M. A.; Afzaal, M.; O'Brien, P. *Chem. Rev.* **2010**, *110*, 4417.
(2) Boudjemline, A.; Islam, M. M.; Louail, L.; Diawara, B. *Physica B* **2011**, *406*, 4272 and references therein.
(3) Osugi, J.; Shimizu, B.; Tanaka, Y.; Kadono, K. *Rev. Phys. Chem. Jpn.* **1966**, *36*, 54.
(4) Hart, G. L. W.; Zunger, A. *Phys. Rev. B* **2000**, *62*, 13522.
(5) Perri, J. A.; La Placa, S.; Post, B. *Acta Crystallogr.* **1958**, *11*, 310.
(6) Williams, F. V.; Ruehrwein, R. A. *J. Am. Chem. Soc.* **1960**, *82*, 1330.
(7) Naritsuka, S.; Mori, M.; Takeuchi, Y.; Monno, Y.; Maruyama, T. *Phys. Status Solidi C* **2011**, *8*, 291.
(8) Butler, M. A. *J. Appl. Phys.* **1977**, *48*, 1914.
(9) Johnson, E. J. In *Semiconductors and Semimetals*; Willardson, R. K., Beer, A. C., Eds.; Academic Press: New York, 1967; Vol. 3, Chapter 6.
(10) Ku, S. M. *J. Electrochem. Soc.* **1966**, *113*, 813.
(11) Chu, T. L.; Hyslop, A. E. *J. Electrochem. Soc.* **1974**, *121*, 412.
(12) Merabet, M.; Rached, D.; Khenata, R.; Benalia, S.; Abidri, B.; Bettahar, N.; Bin Omran, S. *Physica B* **2011**, *406*, 3247 and references therein.
(13) Cohen, M. L. *Phys. Rev. B* **1991**, *43*, 9126.